ОБЪЕДИНЕННЫЙ
ИНСТИТУТ
ЯДЕРНЫХ
ИССЛЕДОВАНИЙ

Дубна

E2-2000-61

G.N.Afanasiev, V.M.Shilov

ON THE SMOOTHED TAMM PROBLEM

Submitted to «Physica Scripta»

2000

1 Introduction

In 1939, Tamm ([1]) approximately solved the following problem: A point charge is at rest at a fixed point of medium up to some moment $t = -t_0$, after which it exhibits an instantaneous infinite acceleration and moves uniformly with a velocity greater than the light velocity in medium. At the moment $t = t_0$, the charge decelerates instantaneously and come to rest. Later, this problem was qualitatively investigated by Aitken [2] and Lawson [3] and numerically by Ruzicka and Zrelov ([4,5]). The analytic solution of this problem in the absence of dispersion was found in [6]. However, in all these studies the information concerning the transition effects was lost due to the instantaneous charge acceleration. The main drawback of the original Tamm problem is instantaneous acceleration and deceleration of a moving charge.

On the other hand, effects arising from unbounded accelerated and decelerated motions of a charge were considered in [7,8]. It was shown there that alongside with the bremsstrahlung and Cherenkov shock waves, a new shock wave arises when the charge velocity coincides with c_n.

The aim of this consideration is to avoid infinite acceleration and deceleration typical for the Tamm problem by applying methods developed in Refs. [7,8]. For this aim, we consider the following charge motion: charge is smoothly accelerated, then moves with a constant velocity, and, finally, is smoothly decelerated.

The plan of our exposition is as follows. In section 2, we recall the notion of moving singularities of the electromagnetic field (EMF) introduced by Schott [9]. Time evolution of EMF singularities for the original and the modified Tamm problems is studied in section 3. In section 4, for the modified Tamm problem, we find angular-frequency distributions of the radiated energy on the sphere of finite radius. Brief account of the results obtained is given in section 5.

2 Moving singularities of electromagnetic field

Let a point charge move inside the medium with polarizabilities ϵ and μ along the given trajectory $\vec{\xi}(t)$. Then, its EMF at the observation point (ρ, z) is given by the Lienard-Wiechert potentials (see, e.g., [10])

$$\Phi(\vec{r},t) = \frac{e}{\epsilon}\sum_i \frac{1}{|R_i|}, \quad \vec{A}(\vec{r},t) = \frac{e\mu}{c}\sum_i \frac{\vec{v}_i}{|R_i|}, \quad div\vec{A} + \frac{\epsilon\mu}{c}\dot{\Phi} = 0\,. \tag{2.1}$$

Here

$$\vec{v}_i = (\frac{d\vec{\xi}}{dt})|_{t=t_i}, \quad R_i = |\vec{r} - \vec{\xi}(t_i)| - \vec{v}_i(\vec{r} - \vec{\xi}(t_i))/c_n\,,$$

and c_n is the light velocity inside the medium ($c_n = c/n, \quad n = \sqrt{\epsilon\mu}$). Summation in (2.1) runs over all physical roots of the equation

$$c_n(t - t') = |\vec{r} - \vec{\xi}(t')|\,. \tag{2.2}$$

To preserve the causality, the radiation retarded time t' should be smaller than the observation time t. Obviously, t' depends on the coordinates $\vec{r}, t$ of the observation point P. With the account of (2.2), one gets for R_i

$$R_i = c_n(t - t_i) - \vec{v}_i(\vec{r} - \vec{\xi}(t_i))/c_n\,. \tag{2.3}$$

To investigate space-time distribution of EMF of a moving charge, one should find (for given $\vec{r}, t$) the retarded times from Eq.(2.2) and substitute them into (2.1).
There is another much simpler method (suggested by Schott [9]) to recover EMF singularities. We seek zeros of the denominators R_i entering into the definition of electromagnetic potentials (2.1). They are obtained from the equation

$$c_n(t-t') = \frac{v(t')}{c_n}(z - \xi(t')). \tag{2.4}$$

Finding t' from (2.4) and substituting it into (2.2), we find the surfaces $\rho(z,t)$ carrying the singularities of the electromagnetic potentials. The equivalence of this approach to the complete solution of (2.1) was proved in [7], where the complete description of EMF for a moving charge was given. It was shown there that the electromagnetic potentials exhibit infinite jumps, when one crosses the above singularity surfaces. Correspondingly, field strengths have δ-type singularities on these surfaces, while the space-time propagation of these surfaces describes the propagation of the radiated energy flux.

3 Time evolution of EMF singularities

We consider the following problem (Fig. 1). A point charge is at rest at a point $-z_0$ of the z axis up to a moment $t = -t_0$. In the time interval $-t_0 < t < -t_1$ (on the space interval $-z_0 < z < -z_1$), the charge moves with acceleration according to the law

$$\xi(t) = -z_0 + \frac{1}{2}a(t+t_0)^2 \tag{3.1}$$

with the velocity $v(t) = a(t+t_0)$. In the time interval $-t_1 < t < t_1$ (on the space interval $-z_1 < z < z_1$), charge moves uniformly

$$\xi(t) = vt. \tag{3.2}$$

In the time interval $t_1 < t < t_0$ (on the space interval $z_0 < z < z_1$), charge moves with deceleration according to the law

$$\xi(t) = z_0 - a(t-t_0)^2/2 \tag{3.3}$$

with the velocity $v(t) = a(t_0 - t)$. Finally, for $t > t_0$, it is again at rest at the point $z = z_0$.
The sewing conditions for trajectories and velocities at $z = \pm z_1$ define t_0, t_1 and a:

$$t_0 = \frac{2z_0 - z_1}{v}, \quad t_1 = \frac{z_1}{v}, \quad a = \frac{v^2}{2(z_0 - z_1)}.$$

In concrete calculations, we deal with dimensionless variables

$$\tilde{t} = ct/z_0, \quad \tilde{t}' = ct'/z_0, \quad \tilde{z} = z/z_0, \quad \tilde{\xi} = \xi/z_0, \quad \tilde{\rho} = \rho/z_0.$$

For brevity, we omit *tilde* signs in obvious cases. Then, Eqs. (2.2) and (2.4) take the form

$$t - t' = n^2\beta(t')(z - \xi(t')), \quad t - t' = n\sqrt{\rho^2 + (z - \xi(t'))^2}. \tag{3.4}$$

We rewrite the second of them in the form

$$\rho^2 = (t - t')^2/n^2 - (z - \xi(t'))^2. \tag{3.5}$$

Finding t' from the first equation (3.4) and substituting it into (3.5), we find the surfaces on which the electromagnetic potentials are singular.

Before going to numerical examples, we consider the time evolution of a moving singularity in the original Tamm problem (Fig.2). Its position at the moment t is given by ([6])

$$\rho = (vt - z)\gamma_n, \quad \gamma_n = 1/\sqrt{\beta_n^2 - 1}, \quad \beta_n = v/c_n,$$

where z changes from $z = z_1^0$ to $z = vt$ for $-z_0/v < t < z_0/v$ and from $z = z_1^0$ to $z = z_2^0$ for $t > z_0/v$. Here

$$z_{1,2}^0 = \frac{ct}{\beta n^2} \pm z_0(\frac{1}{\beta n^2} - 1)$$

(it is assumed, therefore, that $\beta_n > 1$). The singulariry is created at the moment $t = -z_0/v$. In the time interval $-z_0/v < t < z_0/v$, it is enclosed between the current position of the charge on the z axis and the line $\rho = (z + 1)/\gamma_n$. Its head part attached to the charge moves with the velocity v. For $t > z_0/v$, the singularity lying between the lines $\rho = (z - 1)/\gamma_n$ and $\rho = (z + 1)/\gamma_n$ propagates with velocity c_n in the direction inclined under the angle $\theta_{Ch} = \arccos(1/\beta_n)$ towards the motion axis (Fig. 2).

We turn now to a more general case shown in Fig.1. The EMF singularity is created at the moment

$$t = -t_L, \quad t_L = \frac{z_0}{v}[2(1 - x_1)(1 - \frac{1}{\beta_n}) + x_1], \quad x_1 = z_1/z_0$$

when the charge velocity coincides with c_n (Fig. 3). At this moment, the charge is at the point

$$z = -z_L, \quad z_L = \frac{z_0(\beta_n^2 - 1) + z_1}{\beta_n^2} \tag{3.6}$$

of the motion axis. The singularity represents itself a complex consisting of two shock waves. One of them is the usual Cherenkov shock wave propagating with the charge velocity. The normal to it has an angle $\theta_{Ch} = \arccos(1/\beta_n(t))$, $\beta_n(t) = v(t)/c_n$ with the motion axis. The other shock wave, closing the Cherenkov cone, propagates with the velocity c_n. With a good accuracy, it can be approximated by a part of the spherical wave emitted at the moment $t = -t_L$ from the point $z = -z_L$. As time goes, the dimension of this complex grows. The angle θ_{Ch} increases in the time interval $-t_L < t < -t_1$ and remains the same for $-t_1 < t < t_1$. For $t_1 < t < t_L$, the angle θ_{Ch} decreases. For $t = t_L$ (when the charge velocity again coincides with c_n), the Cherenkov shock wave intersects the motion axis under the right angle, and this holds so at subsequent times. After the moment $t = t_L$, the above complex detaches from the charge and propagates with the velocity c_n. This demonstrates Fig. 3, where the time evolution of EMF singularities is shown for $z_1/z_0 = 0.5$. It should be noted that, contrary to the original Tamm problem corresponding to $z_1 = z_0$ (Fig.2), moving singularities for $z_1 < z_0$ are distributed over a much larger angular region, no matter how small is deviation of z_0 from z_1. This is due to accelerated and decelerated motion of the charge on the intervals $-z_0 < z < -z_1$ and $z_1 < z < z_0$. This illustrates also Fig. 4, where the time evolution of EMF singularities is shown for $z_1/z_0 = 0.99$.

Since in the original Tamm problem the transition from the state of rest to the state of motion is instantaneous, the above complex degenerates into a segment propagating with the velocity c_n (Fig. 2).

4 Frequency distribution of the electromagnetic radiation

However, usually, experimentalists measure not the EMF distribution at a given moment of time, integrated over all radiated frequencies, but the EMF energy flux with a given frequency for the whole time of charge motion. For this, we need the Fourier component of the vector potential:

$$A_\omega = \frac{1}{c}\int dV' \frac{1}{R} j_\omega(x', y', z') \exp(-\omega R/c_n), \tag{4.1}$$

where $R = [(x-x')^2 + (y-y')^2 + (z-z')^2]^{1/2}$ and j_ω is the Fourier component of the current density

$$j_\omega(\vec{r}) = \frac{1}{2\pi}\int dt \exp(-i\omega t) j(\vec{r}, t), \quad j(\vec{r}, t) = ev(t)\delta(x)\delta(y)\delta(z - \xi(t)).$$

Substituting here $\xi(t)$ and $v(t)$ given by Eqs. (3.1)-(3.3), one obtains

$$j_\omega = \frac{e}{2\pi}\delta(x)\delta(y)\{\Theta(z+z_0)\Theta(-z-z_1)\exp[\frac{i\omega}{v}(2z_0 - z_1 - 2\sqrt{(z+z_0)(z_0-z_1)})]+$$

$$+\Theta(z+z_1)\Theta(z_1-z)\exp(-\frac{i\omega z}{v})+$$

$$+\Theta(z_0-z)\Theta(z-z_1)\exp[-\frac{i\omega}{v}(2z_0 - z_1 - 2\sqrt{(z_0-z)(z_0-z_1)})]\}.$$

This leads to the following vector potential on the sphere of radius R_0

$$A_\omega = \frac{e\epsilon_0}{2\pi c}\int_{-1}^{-x_1}\frac{dz'}{R}\exp\{-\frac{i\omega z_0}{v}[2\sqrt{(z'+1)(1-x_1)} - 2 + x_1] - ik_n R_0 R\}+$$

$$+\frac{e\epsilon_0}{2\pi c}\int_{-x_1}^{x_1}\frac{dz'}{R}\exp(\frac{-i\omega z_0}{v} - ik_n R_0 R)+$$

$$\frac{e\epsilon_0}{2\pi c}\int_{x_1}^{1}\frac{dz'}{R}\exp\{\frac{-i\omega z_0}{v}[-2\sqrt{(1-z')(1-x_1)} + 2 - x_1] - ik_n R R_0\}. \tag{4.2}$$

Here $k_n = \omega/c_n$, $R = [1 - 2\epsilon_0 z'\cos\theta + \epsilon_0^2 z'^2]^{1/2}$, $\epsilon_0 = z_0/R_0$, $x_1 = z_1/z_0$; θ is the polar angle of the observation point. Using A_ω, we evaluate Fourier components of EMF

strengths and the energy flux through the unit solid angle of the sphere of radius R_0 for the whole time of charge motion

$$\frac{dW}{d\Omega} = \frac{c}{4\pi} R_0^2 \int\limits_{-\infty}^{\infty} dt (\vec{E} \times \vec{H})_r$$

(subscript r means a radial component of $(\vec{E} \times \vec{H})$). Expressing $\vec{E}$ and $\vec{H}$ through their Fourier transforms

$$\vec{E} = \int \exp(i\omega t)\vec{E}_\omega d\omega, \quad \vec{H} = \int \exp(i\omega t)\vec{H}_\omega d\omega$$

and integrating over t, one gets

$$\frac{dW}{d\Omega} = \frac{cR_0^2}{2} \int\limits_{-\infty}^{\infty} (\vec{E}(\omega) \times \vec{H}(-\omega)) d\omega = \int\limits_0^{\infty} S(\omega) d\omega, \tag{4.3}$$

where

$$S(\omega, \theta) = \frac{d^2 W}{d\omega d\Omega} = cR_0^2 [\vec{E}_\theta^{(r)}(\omega)\vec{H}_\phi^{(r)}(\omega) + \vec{E}_\theta^{(i)}(\omega)\vec{H}_\phi^{(i)}(\omega)]. \tag{4.4}$$

This quantity shows how the Fourier component of the energy radiated for the whole time of charge motion is distributed over the sphere S. It does not depend on time. The superscripts (r) and (i) mean the real and imaginary parts of $E_\theta(\omega)$ and $H_\phi(\omega)$. After rather lengthy, although straightforward calculations, one gets

$$S(\omega, \theta) = \frac{d^2 E}{d\omega d\Omega} = \frac{e^2 k^2 z_0^2 n}{4\pi^2 c} \sin^2\theta (I_c I_c' + I_s I_s'), \tag{4.5}$$

where

$$I_c = \sum_{i=1}^{3} I_c(i), \quad I_c' = \sum_{i=1}^{3} I_c'(i), \quad I_s = \sum_{i=1}^{3} I_s(i), \quad I_s' = \sum_{i=1}^{3} I_s'(i), \tag{4.6}$$

$$I_s(1) = \int\limits_{-1}^{-x_1} \frac{\sin\psi_1}{R^2} dz', \quad I_s(2) = \int\limits_{-x_1}^{x_1} \frac{\sin\psi_2}{R^2} dz', \quad I_s(3) = \int\limits_{x_1}^{1} \frac{\sin\psi_3}{R^2} dz',$$

$$I_c(1) = \int\limits_{-1}^{-x_1} \frac{\cos\psi_1}{R^2} dz', \quad I_c(2) = \int\limits_{-x_1}^{x_1} \frac{\cos\psi_2}{R^2} dz', \quad I_c(3) = \int\limits_{x_1}^{1} \frac{\cos\psi_3}{R^2} dz',$$

$$I_s'(1) = \int\limits_{-1}^{-x_1} \frac{\sin\psi_1}{R^3} (1 - z'\epsilon_0 \cos\theta) dz', \quad I_s'(2) = \int\limits_{-x_1}^{x_1} \frac{\sin\psi_2}{R^3} (1 - z'\epsilon_0 \cos\theta) dz',$$

$$I_s'(3) = \int\limits_{x_1}^{1} \frac{\sin\psi_3}{R^3} (1 - z'\epsilon_0 \cos\theta) dz', \quad I_c'(1) = \int\limits_{-1}^{-x_1} \frac{\cos\psi_1}{R^3} (1 - z'\epsilon_0 \cos\theta) dz',$$

$$I_c'(2) = \int\limits_{-x_1}^{x_1} \frac{\cos\psi_2}{R^3} (1 - z'\epsilon_0 \cos\theta) dz', \quad I_c'(3) = \int\limits_{x_1}^{1} \frac{\cos\psi_3}{R^3} (1 - z'\epsilon_0 \cos\theta) dz'.$$

Here

$$\psi_1 = \frac{\omega z_0}{v}[2\sqrt{(1+z')(1-x_1)} - 2 + x_1] + k_n R_0(R-1), \quad \psi_2 = \frac{\omega z_0}{v} z' + k_n R_0(R-1),$$

$$\psi_3 = -\frac{\omega z_0}{v}[2\sqrt{(1-z')(1-x_1)} - 2 + x_1] + k_n R_0(R-1). \tag{4.7}$$

When obtaining (4.6), we neglected terms of the order $1/k_n R_0$ and higher outside the ψ_1, ψ_2, and ψ_3 functions. In the optical diapason (where the Cherenkov radiation is observed), the quantity $1/k_n R_0$ is about 10^{-7} for $R_0 = 1cm$. Therefore, our approximation is justified with a good accuracy.
Before going to numerical results, consider the limiting cases.

4.1 Large observation distances, finite acceleration

Large distances mean that the following conditions are fulfilled

$$z_0 << R_0, \quad k_n R_0 >> 1, \quad k_n z_0^2/R_0 << 1. \tag{4.8}$$

Under these conditions, the radiation intensity in the Tamm original problem corresponding to instantaneous charge acceleration at $z = \pm z_0$ and uniform motion for $-z_0 < z < z_0$ is given by the famous Tamm formula

$$\frac{d^2\mathcal{E}}{d\Omega d\omega} = \frac{e^2}{\pi^2 cn}[\sin\theta \frac{\sin\omega t_0(1-\beta_n\cos\theta)}{\cos\theta - 1/\beta_n}]^2, \quad t_0 = \frac{z_0}{v}. \tag{4.9}$$

This formula is frequently used by experimentalists (see, e.g., [11-13]) for the identification of Cherenkov radiation. To satisfy conditions (4.8), it is enough that $R_0 \to \infty$ in (4.5). Then,

$$I_s = I_s' = \sum_{i=1}^{3} I_s(i), \quad I_c = I_c' = \sum_{i=1}^{3} I_c(i), \tag{4.10}$$

$$I_s(1) = I_s'(1) = \int_{-1}^{-x_1} \sin\psi_1 dz', \quad I_c(1) = I_c'(1) = \int_{-1}^{-x_1} \cos\psi_1 dz',$$

$$I_s(2) = I_s'(2) = 0, \quad I_c(2) = I_c'(2) = \frac{2}{k_n z_0} \frac{\sin[k_n z_1(\cos\theta - 1/\beta_n)]}{\cos\theta - 1/\beta_n},$$

$$I_s(3) = I_s'(3) = \int_{x_1}^{1} \sin\psi_3 dz', \quad I_c(3) = I_c'(3) = \int_{x_1}^{1} \cos\psi_3 dz',$$

where

$$\psi_1 = \frac{\omega z_0}{v}[2\sqrt{(1+z')(1-x_1)} - 2 + x_1] - k_n z_0 z'\cos\theta, \quad \psi_2 = \frac{\omega z_0}{v} z'(1-\beta_n\cos\theta),$$

$$\psi_3 = -\frac{\omega z_0}{v}[2\sqrt{(1-z')(1-x_1)} - 2 + x_1] - k_n z_0 z'\cos\theta. \tag{4.11}$$

Equation (4.5) with such I_s describes the radiation intensity on the sphere of infinite radius arising from charge motion defined by (3.1)-(3.3). For $z_1 = z_0$, one gets

$$I_s(1) = I_s(3) = I_c(1) = I_c(3) = 0, \quad I_s(2) = \int_{-1}^{1} \sin\psi_2 dz' = 0,$$

$$I_c(2) = \int_{-1}^{1} \cos\psi_2 dz' = \frac{2}{k_n z_0} \frac{\sin[k_n z_0(\cos\theta - 1/\beta_n)}{\cos\theta - 1/\beta_n},$$

thus, recovering Tamm's intensity (4.9).
Fig. 5 shows radiation intensities (4.5) with I_c and I_s given by (4.10) for $z_1 = z_0$ (a), $z_1 = 0.5z_0$ (b), $z_1 = 0.1z_0$ (c) and $z_1 = 0$ (d). Obviously, case (a) corresponds to the Tamm original problem. There is no maximum in the neigbourhood of Cherenkov angle for Fig. 5,d describing accelerated motion without horizontal part of the charge trajectory (see Fig.1).

4.2 Finite observation distances, instantaneous acceleration

Let $z_1 = z_0$. This corresponds to the uniform charge motion on the interval $-z_0 < z < z_0$. Then,

$$I_s(1) = I_s(3) = I_c(1) = I_c(3) = I'_s(1) = I'_s(3) = I'_c(1) = I'_c(3) = 0,$$

$$I_s(2) = \int_{-1}^{1} \frac{\sin\psi_2}{R^2} dz', \quad I_c(2) = \int_{-1}^{1} \frac{\cos\psi_2}{R^2} dz',$$

$$I'_s(2) = \int_{-1}^{1} \frac{\sin\psi_2}{R^3}(1 - z'\epsilon_0\cos\theta)dz', \quad I'_c(2) = \int_{-1}^{1} \frac{\cos\psi_2}{R^3}(1 - z'\epsilon_0\cos\theta)dz', \qquad (4.12)$$

where ψ_2 is the same as in (4.7). Intensity (4.5) with

$$I_s = I_s(2), \quad I_c = I_c(2), \quad I'_s = I'_s(2), \quad I'_c = I'_c(2)$$

shows how the energy flux radiated by a charge uniformly moving on the interval $(-z_0, z_0)$ is distributed over the sphere of finite radius R_0. This case was considered in detail in [14]. It was shown there that in typical experimental situations, the last of conditions (4.8) is not fulfilled. In this case, one should use either Eqs. (4.5) with I_c, I_s given by (4.10) or an analytic formulae obtained in [14]. If, in addition to $z_1 = 1$, the radius R_0 of the observation sphere tends to infinity, one gets

$$\epsilon_0 \to 0, \quad k_n R_0(R-1) \to -k_n z_0 z' \cos\theta, \quad \psi_2 \to k_n z_0 z'(\frac{1}{\beta_n} - \cos\theta).$$

In this case, Eq.(4.5) is again reduced to the Tamm formula (4.9).

4.3 Finite observation distances, finite acceleration

The angular dependences (4.5) with I and I' given by (4.6) on the sphere of radius $R_0 = 1m$ are shown in Fig. 6 for different horizontal parts of the charge trajectory: $z_1/z_0 = 1$ (a), $z_1/z_0 = 0.5$ (b), $z_1/z_0 = 0.1$ (c) and $z_1/z_0 = 0$ (d). Obviously, Fig.6 (a) corresponds to the intensity of the original Tamm problem on the sphere of radius $R_0 = 1m$. It is distributed over a much larger angular interval and is much smaller than the intensity described by the Tamm formula (4.8) corresponding to $R_0 = \infty$ (see Fig. 5 a). As in Fig. 5 d, there in no pronounced maximum in the neighbourhood of Cherenkov angle in the absence of horizontal part of the trajectory (Fig. 6 d).

5 Conclusion

We modified the Tamm problem describing the charge motion on a finite space interval by introducing smooth acceleration and deceleration of a moving charge. The space distribution of the electromagnetic field singularities is studied. When the charge velocity coincides with the velocity of light in medium, a new shock wave (in addition to the Cherenkov shock wave) arises that propagates with the velocity of light in medium.
The angular-frequency distribution of the emitted radiation crucially depends on the radius of the sphere, on which the observations are made. This should be taken into account when describing the results of the Cherenkov-like experiments.

Acknowledgement

The authors are indebted to Prof. V.P. Zrelov and Prof. J. Ruzicka for many stimulating and interesting discussions.

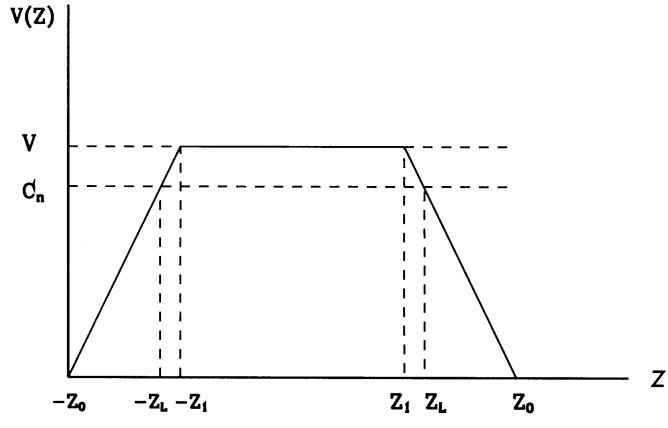

Figure 1: Schematic presentation of the modified Tamm model. Charge accelerates, moves uniformly with the velocity v and decelerates on the intervals $(-z_0, -z_1)$, $(-z_1, z_1)$ and (z_1, z_0), resp. The velocity of light in medium c_n is reached at the points $\mp z_L$ of the motion axis.

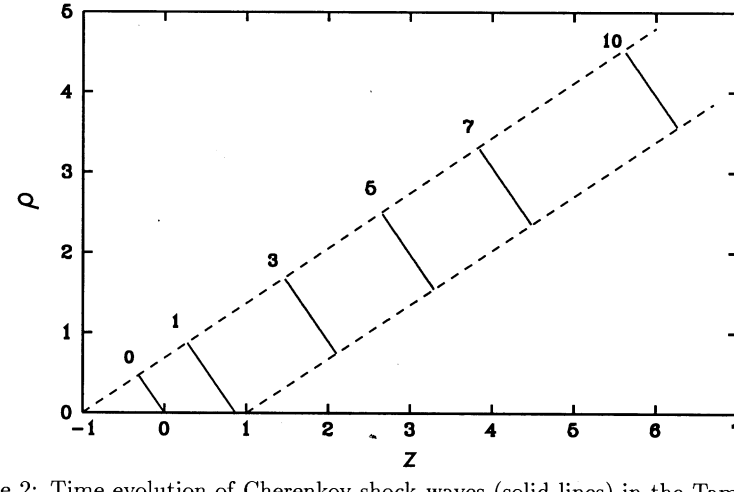

Figure 2: Time evolution of Cherenkov shock waves (solid lines) in the Tamm original problem. Numbers of them mean laboratory time. The Cherenkov shock wave propagates with the velocity c_n between two dotted lines (see the text); z and ρ in units z_0, t in units z_0/c.

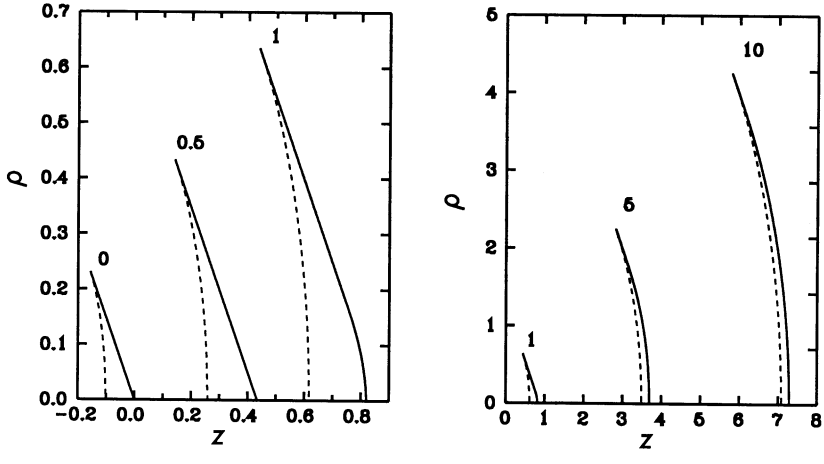

Figure 3: Time evolution of EMF singularities in the Tamm modified problem (see Fig. 1) for $z_1/z_0 = 0.5$ and $\beta_n \approx 1.21$. For these z_1 and β_n, the complex consisting of Cherenkov shock wave (solid line) and the surface closing the Cherenkov cone (dotted line) is created at the point $z = -z_L \approx -0.66$ of the motion axis. At the moment $z = z_L$ this complex detaches from a charge and propagates with the velocity c_n. The charge motion terminates at $z = 1$; z and ρ in units z_0.

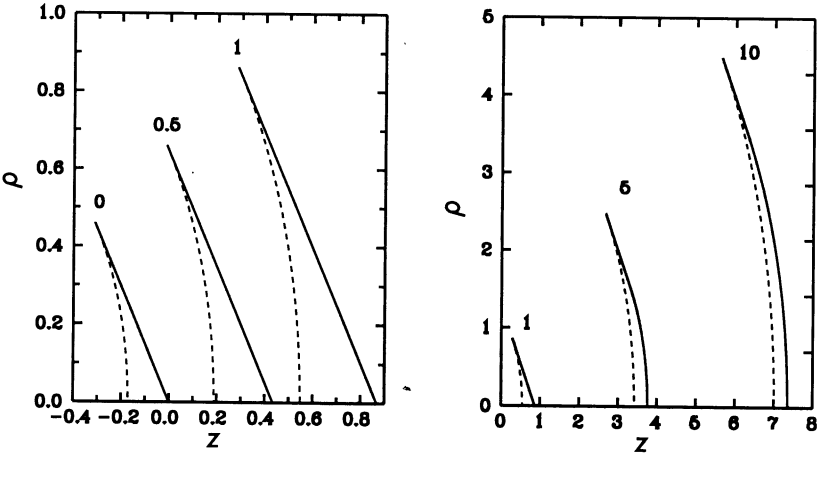

Figure 4: The same as in Fig. 3 but for $z_1/z_0 = 0.99$ that corresponds to $z_L \approx z_0$. Despite the proximity of z_1 to z_0, the distribution of EMF singularities disagrees with ones of the original Tamm problem (for which $z_1 = z_0$) shown in Fig.2.

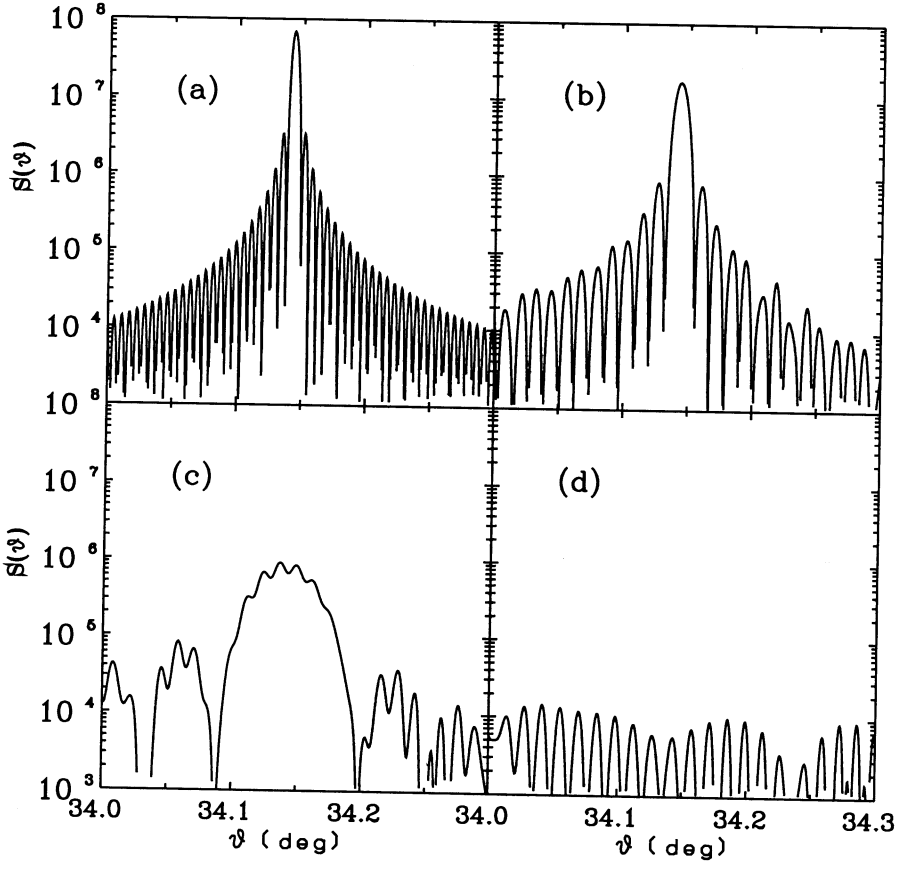

Figure 5: Angular distribution of the radiation intensity (in units e^2/c) in the modified Tamm problem on the sphere of infinite radius for $z_1/z_0 = 1$ (a), $z_1/z_0 = 0.5$ (b), $z_1/z_0 = 0.1$ (c) and $z_1/z_0 = 0$ (d). The charge velocity $\beta = 0.868$, refractive index $n = 1.392$, wavelength $\lambda = 4 \cdot 10^{-5} cm$, the motion interval $2z_0 = 0.5cm$. Distributions (a) and (d) correspond to the original Tamm problem and modified Tamm problem without horizontal part of the charge trajectory, resp.

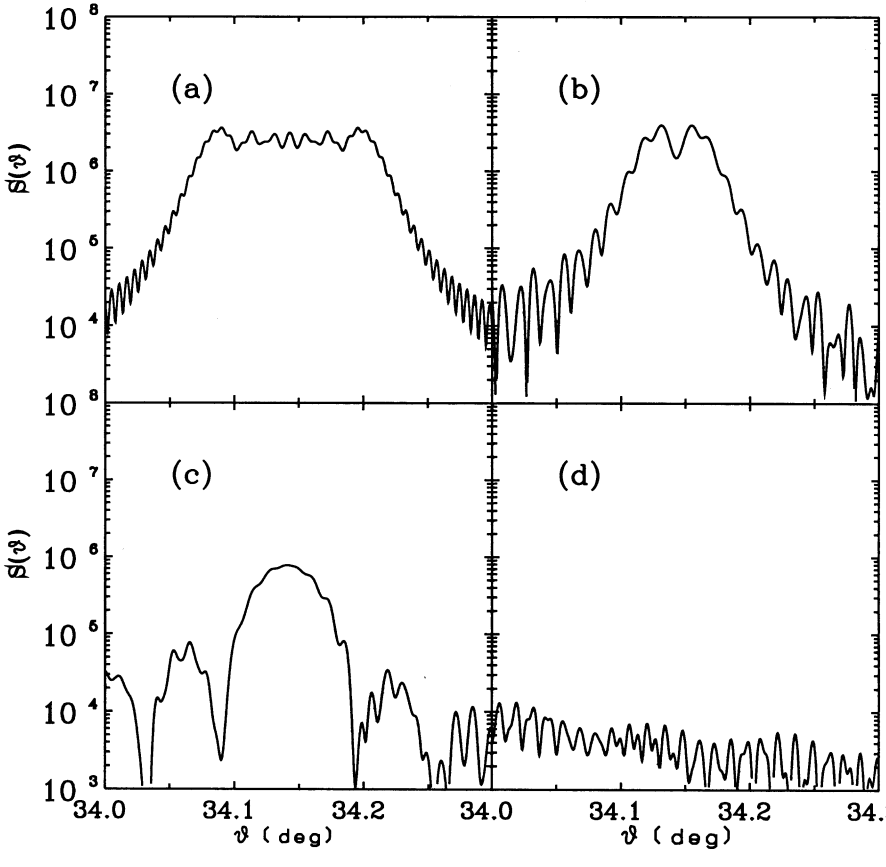

Figure 6: The same as in Fig. 5, but for the radius of the observation sphere $R_0 = 1m$. Comparison with Fig.5 indicates on the strong dependence of intensities on the observation sphere radius R_0.

References

[1] Tamm I.E., J. Phys. USSR 1, No 5-6, 439 (1939).

[2] Aitken D.K. et al., Proc. Phys. Soc., 83, 710 (1963).

[3] Lawson J.D., Phil. Mag., 45, 748 (1954);
Lawson J.D., Amer. J.Phys., 33, 1002 (1965).

[4] Zrelov V.P. and Ruzicka J., Chech. J. Phys., B 39, 368 (1989).

[5] Zrelov V.P. and Ruzicka J., Chech. J. Phys., 42, 45 (1992).

[6] Afanasiev G.N., Beshtoev Kh.M. and Stepanovsky Yu.P., Helv. Phys. Acta, 2,111 (1996); Afanasiev G.N., Kartavenko V.G. and Stepanovsky Yu.P., J.Phys.D: Applied Physics, 32, 2029 (1999).

[7] Afanasiev G.N., Eliseev S.M. and Stepanovsky Yu.P., Proc. Roy. Soc. London, Series A, 454, 1049 (1998).

[8] Afanasiev G.N. and Kartavenko V.G., Can. J. Phys., 77, 561 (1999).

[9] Schott G.A., Electromagnetic Radiation (Cambridge Univ. Press, Cambridge, 1912).

[10] Landau L.D. and Lifshitz E.M., The Classical Theory of Fields (Pergamon, New York, 1962).

[11] Zrelov V.P., Vavilov-Cherenkov Radiation in High-Energy Physics (Jerusalem, Israel Program for Scientific Translations, 1970).

[12] Frank I.M., Vavilov-Cherenkov Radiation (Nauka, Moscow, 1988).

[13] Jelly J.V., Cherenkov Radiation and its Applications (Pergamon, London, 1958).

[14] Afanasiev G.N. and Kartavenko V.G., 2000, JINR Preprint E2-17-2000, Dubna;
Afanasiev G.N. and Shilov V.M., 2000, JINR Preprint E2-34-2000, Dubna.

Received by Publishing Department
on March 20, 2000.

Афанасьев Г.Н., Шилов В.М.
Е2-2000-61

О сглаженной задаче Тамма

Чтобы снять возражения против мгновенного ускорения и замедления движения заряда в задаче Тамма, рассматривается движение заряда с конечными ускорением и замедлением. При этом, в дополнение к ударной волне черенковского излучения, появляется новая ударная волна в тот момент, когда скорость заряда совпадает со скоростью света в веществе. Угловое распределение излучения существенно зависит от радиуса сферы, на которой проводятся наблюдения.

Работа выполнена в Лаборатории теоретической физики им. Н.Н.Боголюбова ОИЯИ.

Препринт Объединенного института ядерных исследований. Дубна, 2000

Afanasiev G.N., Shilov V.M.
E2-2000-61

On the Smoothed Tamm Problem

To remove obstacles against an instantaneous acceleration and deceleration of charge in the Tamm problem, we consider charge motion on a finite space interval with finite acceleration and deceleration. When the charge velocity coincides with the velocity of light in medium, a new shock wave (in addition to the Cherenkov shock wave) arises which propagates with the light velocity in medium. The angular distribution of the emitted radiation crucially depends on the radius of the sphere on which the observations are made.

The investigation has been performed at the Bogoliubov Laboratory of Theoretical Physics, JINR.

Preprint of the Joint Institute for Nuclear Research. Dubna, 2000

Макет Т.Е.Попеко

Подписано в печать 17.04.2000
Формат 60 × 90/16. Офсетная печать. Уч.-изд. листов 1,52
Тираж 425. Заказ 51982. Цена 1 р. 82 к.

Издательский отдел Объединенного института ядерных исследований
Дубна Московской области